Doped Graphene as Tunable Electron−Phonon Coupling Material

Claudio Attaccalite,*,[†],[‡] Ludger Wirtz,[§] Michele Lazzeri,[||] Francesco Mauri,[||] and Angel Rubio[†],[⊥]

[†]Nano-Bio Spectroscopy group and ETSF Scientific Development Centre, Dpto. Fisica de Materiales, Universidad del Pais Vasco, Centro de Fisica de Materiales CSIC-UPV/EHU-MPC and DIP, E-20018 San Sebastian, Spain, [‡]Institut Neel, CNRS-UJF, Grenoble, France, [§]Institute for Electronics, Microelectronics, and Nanotechnology, CNRS-UMR 8520, Dept. ISEN, B.P. 60069, 59652 Villeneuve d'Ascq Cedex, France, [||]IMPMC, Universités Paris 6 et 7, CNRS, IPGP, 140 rue de Lourmel, 75015 Paris, France, and [⊥]Fritz-Haber-Institut der Max-Planck-Gesellschaft, Berlin, Germany

ABSTRACT We present a new way to tune the electron−phonon coupling (EPC) in graphene by changing the deformation potential with electron/hole doping. We show the EPC for highest optical branch at the high symmetry point K acquires a strong dependency on the doping level due to electron−electron correlation not accounted in mean-field approaches. Such a dependency influences the dispersion (with respect to the laser energy) of the Raman D and 2D lines and the splitting of the 2D peak in multilayer graphene. Finally this doping dependence opens the possibility to construct tunable electronic devices through external control of the EPC.

KEYWORDS Graphene, electron−phonon coupling, Raman spectroscopy

A large amount of work envisioning exciting new applications of graphene-based devices in nanoelectronics has been published in the last years (see ref 1 and references therein). The performance of those electro-optical graphene-based devices[2] is governed to a large extent by electron−phonon coupling (EPC) or, more precisely, by the deformation potential. For example in high-current transport the scattering with phonons increases the differential resistance in carbon nanotubes and graphene.[3−5] It has been widely assumed that the deformation potential in graphene is constant with respect to the electron/hole concentration. For a proper description of device performances, it is necessary to control the validity of this approximation. Indeed, here we show that the deformation potential displays a rather strong doping dependence which should be taken into account in the design of new graphene devices.

The interaction between electrons and phonons in graphene and graphite has been studied with many experimental techniques ranging from angle-resolved photoemission spectroscopy (ARPES),[7] inelastic X-ray scattering (IXS),[8] scanning tunneling spectroscopy (STS)[9] to Raman spectroscopy.[10] In particular, Raman spectroscopy is commonly employed in graphene characterization because it is sensitive to the number of layers,[11,12] the doping level,[13−18] and the graphene edges.[19] In order to interpret all above-mentioned experiments, a complete knowledge of the electronic structure, the phonon dispersion, and the electron−phonon interaction

is required. In graphene the electron−phonon coupling (EPC) between the π and π^* bands to different phonon modes is responsible for the peculiar properties observed in the experiments.[20,21,23]

The dimensionless electron−phonon coupling for a mode ν at momentum $\mathbf{q}$ is given by

$$\lambda_{\mathbf{q}\nu} = \frac{2}{\hbar\omega_{\mathbf{q}\nu}N_\sigma(\epsilon_f)} \int_{BZ} \frac{d\mathbf{k}}{\Omega} \sum_{i,j} |g^\nu_{\mathbf{k}i,(\mathbf{k}+\mathbf{q})j}|^2 \delta(\epsilon_k - \epsilon_f)\cdot\delta(\epsilon_{k+q} - \epsilon_f)$$

(1)

where $\omega_{q\nu}$ is the phonon frequency, $N_\sigma(\epsilon_f)$ is the density of states per spin channel at the Fermi level, and i and j are band indices. The term

$$g^\nu_{\mathbf{k}i,(\mathbf{k}+\mathbf{q})j} = \langle \mathbf{k} + \mathbf{q}, j | \Delta V_{\mathbf{q}\nu} | \mathbf{k}, i \rangle \sqrt{\hbar/(2M\omega_{q\nu})}$$

(2)

is the electron−phonon coupling matrix element that describes the scattering of an electron from band i to band j due to the phonon ν with wavevector $\mathbf{q}$. The quantity $\lambda_{\mathbf{q}\nu}$ depends on the doping of the system through the shift of the Fermi level and the subsequent change in $N_\sigma(\epsilon_f)$. Furthermore, it (weakly) depends on the doping through the variation of $g^\nu_{\mathbf{k}i,(\mathbf{k}+\mathbf{q})j}$. In the following we are interested in the contribution coming from the matrix elements, therefore, in order to lift the dependence on the phonon frequency, we calculate directly $\langle \mathbf{k} + \mathbf{q}, j | \Delta V_{q\nu} | \mathbf{k}, i \rangle$. In particular, we will concentrate on the coupling of the π and π^* bands with the highest optical phonon branch (HOB) at Γ (E_{2g} mode) and at K (A_1' mode). We define

$$\langle D_\Gamma^2 \rangle = \sum_{i,j}^{\pi,\pi^*} |\langle \mathbf{K}, j | \Delta V_{\Gamma E_{2g}} | \mathbf{K}, i \rangle|^2 / 4 \qquad (3)$$

and

$$\langle D_{\mathbf{K}}^2 \rangle_{\mathbf{k}}^{\pi\pi^*} = |\langle 2\mathbf{K} + \mathbf{k}, \pi^* | \Delta V_{\mathbf{K}A_1'} | \mathbf{K} + \mathbf{k}, \pi \rangle|^2 / 2 \qquad (4)$$

where the sums are performed over the two times degenerate π bands at $\mathbf{K}$. In the limit of zero doping, $\langle D_\Gamma^2 \rangle$ is equal to $\langle D_\Gamma^2 \rangle_F$ as defined in ref 27. In the limit of zero doping and $\mathbf{k} \rightarrow \mathbf{0}$, $\langle D_{\mathbf{K}}^2 \rangle_{\mathbf{k}}^{\pi\pi^*}$ is equal to $\langle D_{\mathbf{K}}^2 \rangle_F$ as defined in ref 27. In fact, for small $\mathbf{k}$ the matrix elements between π and π (or between π^* and π^*) are zero (see note[24] of ref 23). In our earlier publications[27] we called these quantities electron−phonon coupling. In view of the above definitions (eqs 1 and 2) it is more precise to call $\langle D_\Gamma^2 \rangle$ and $\langle D_{\mathbf{K}}^2 \rangle_{\mathbf{k}}^{\pi\pi^*}$ the "square of the deformation potential" (or, to be very precise, the "average squared deformation potential of the π bands"). We focus our attention on $\langle D_\Gamma^2 \rangle$ and $\langle D_{\mathbf{K}}^2 \rangle_{\mathbf{k}}^{\pi\pi^*}$, because these two quantities are the ones responsible for the intensity and position of the peaks in Raman spectroscopy,[10] the kinks in ARPES, and the phonon slope close to the Kohn anomalies.[23]

In graphene and carbon nanotubes, the deformation potential has been usually obtained from tight-binding Hamiltonians computing the change in the nearest-neighbor hopping energy due to a lattice distortion.[24] In this approach the deformation potential has been always considered a constant with respect to the electron or hole density. This approximation, although not justified microscopically, is widely used.[1,13,14,16,18,20,24,26] Moreover even ab initio calculations using density functional theory (DFT) in the local density approximation (LDA) apparently confirmed that the deformation potential is weakly dependent on doping. However, including effects of electron−electron correlation, we will show that for the $\mathbf{K}$ (A_1' mode) mode, this approximation breaks down and $\langle D_{\mathbf{K}}^2 \rangle_{\mathbf{k}}^{\pi\pi^*}$ can change by more than 40% just varying the electronic distribution (i.e., gated single and multilayer graphene). This fact can be directly probed measuring the Raman D-peak dispersion of graphene versus doping as we will discuss in the following.

Recently it has been proven[27,28] that in (neutral) graphene $\langle D_{\mathbf{K}}^2 \rangle_{\mathbf{k}=0}^{\pi\pi^*}$ is strongly affected by electron correlation. In our previous work,[27] we have shown that DFT-LDA or DFT-GGA underestimates $\langle D_{\mathbf{K}}^2 \rangle_{\mathbf{k}=0}^{\pi\pi^*}$ by almost a factor of 2. The electron−electron correlation can be included on the level of the GW approximation obtaining a deformation potential which reproduces the Raman D-line dispersion and the phonon slope around $\mathbf{K}$ within a few percent.[8] On the contrary, the deformation potential of the $\Gamma-E_{2g}$ mode was shown to depend very little on electron−electron correlation.[27] In this Letter, we use the GW approximation to calculate the variation of the deformation potential with doping.
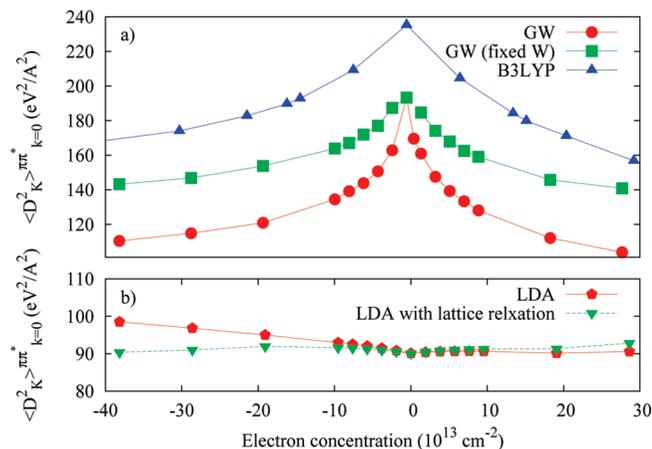

FIGURE 1. (a) Squared deformation potential for the $\mathbf{K}-A_1'$ phonon between the π bands $\langle D_{\mathbf{K}}^2 \rangle_{\mathbf{k}=0}^{\pi\pi^*}$ in different approximations. Circles are GW results; squares are GW(0), keeping the screened potential $W(0)$ fixed to the undoped case; triangles are B3LYP results. (b) Variation of $\langle D_{\mathbf{K}}^2 \rangle_{\mathbf{k}=0}^{\pi\pi^*}$ in LDA approximation, including or not lattice relaxation (triangles and pentagons, respectively).

Doped graphene can be created in single layer field-effect transistor (FET) based experiments, where an electron concentration up to 3×10^{13} cm^{-2} electron can be realized, while higher dopings are obtained using intercaled graphite.[29] In order to simulate doped graphene, we employed a slab-geometry, i.e., bulk geometry with large distance between the layers, changing the number of electrons in the unit cell and then compensating the negative/positive charge with a uniform positive/negative background, see ref 30 for details. The electronic and phonon structure of graphene at different doping levels were computed using DFT-LDA. The deformation potential is obtained using the scheme proposed in ref 27 based on a *frozen-phonon* approach by looking at the modification of the electronic structure upon displacement of the atoms following a given normal mode. The major advantage of this approach is that it can be used with electronic structure methods other than DFT. When DFT is used, this approach gives the same result of density functional perturbation theory. First of all, we investigated the effect of the change in the lattice constant a, induced by the doping, on the deformation potential. Using the functional dependence of a versus the electron concentration from eq 2 of ref 31, we calculated the deformation potential for different doping level with the corresponding lattice parameters. In panel b of Figure 1 we compare the deformation potential calculated with and without lattice relaxation for different electron/hole doping. The difference between the two results is small when compared with renormalization effects that we are going to describe below. Therefore, in order to make the analysis simpler, we performed all the calculations with the graphene experimental lattice constant.

On the level of the LDA, the variation of $\langle D_{\mathbf{K}}^2 \rangle_{\mathbf{k}}^{\pi\pi^*}$ and $\langle D_\Gamma^2 \rangle$ with doping is very small. In the following, we will introduce correlation effects beyond DFT-LDA on the deformation potential. We included these effects in the GW approxima-

TABLE 1. Squared Deformation Potential for the $K-A_1'$ Phonon versus Doping, in GW Approximation[a]

	graphene		
Δn (10^{13} cm^{-2})	$\langle D^2_{K}\rangle^{\pi\pi^*}_{k=0}$ (eV^2/Å^2)	$\Delta\epsilon_M$ (eV)	D slope (cm^{-1}/eV)
−38.16	110	4.550	27.58
−28.62	115	4.585	29.83
−19.08	121	4.632	32.41
−9.54	135	4.711	37.84
−7.63	139	4.723	39.49
−5.72	144	4.761	41.20
−3.81	151	4.795	43.67
−1.90	163	4.820	48.20
0.00	193	4.867	58.40
1.90	161	4.803	47.82
3.81	148	4.765	43.26
5.72	139	4.724	40.24
7.63	133	4.667	38.44
9.54	128	4.642	36.75
19.08	112	4.532	31.53
28.62	104	4.485	29.11

[a] $\langle D^2_{K}\rangle^{\pi\pi^*}_{k=0}$ and $\Delta\epsilon_M$ are defined in the text, the LDA value of $\Delta\epsilon_M$ at zero doping is 4.01115 eV. D slope is the slope of the Raman D peak dispersion (peak energy versus laser frequency); see the text.

FIGURE 2. Electronic gap at M point ($\Delta\epsilon_M$) as function of doping in different approximations: GW with fixed screened Coulomb interaction, GW, and LDA.

tion[34] that has been successfully applied in the study of graphene and graphite[32,33] and its compounds.[36,37] First of all we studied the doping dependence on the renormalization of the quasi-particle band structure (see also refs 41 and 42), that will be subsequently used to calculate the D-peak dispersion. In Table 1, we report the change in the gap between the π and π^* at the high symmetry point **M**, $\Delta\epsilon_M$, as function of doping. This quantity is directly related to the optical properties of graphite and graphene-based materials, and provides an alternative way to measure quasi-particle renormalization effects. The strongest renormalization effect (compared to the LDA gap) is present for zero doping. Electron/hole doping rapidly decreases the GW renormalization of the quasi-particle band structure. The same is true for the Fermi velocity v_F. Subsequently, from the change in the quasi-particle band structure upon atomic displacement, we calculated $\langle D^2_{K}\rangle^{\pi\pi^*}_{k}$ in the same way as was done for LDA (see ref 27). We found that for $\langle D^2_\Gamma\rangle$ the GW result of ref 27 is mainly unaffected by the doping level.[38] The situation is completely different for $\langle D^2_{K}\rangle^{\pi\pi^*}_{k}$. In Figure 1 and Table 1, we report the value of $\langle D^2_{K}\rangle^{\pi\pi^*}_{k=0}$ as a function of the doping in different approximations. In LDA (panel b) it is almost a constant, but the situation is completely different at the GW level (panel a): $\langle D^2_{K}\rangle^{\pi\pi^*}_{k=0}$ is increased more than 80 % with respect to the LDA result (at zero doping) and it acquires a strong doping dependence. The renormalized deformation potential rapidly decreases with electron or hole doping and gets close to the LDA value at large doping.

In the following, we discuss the origin of the strong doping dependence of $\langle D^2_{K}\rangle^{\pi\pi^*}_{k=0}$ within the GW approximation. Both the Green's function, G, and the screened Coulomb potential, W, are doping dependent. In order to disentangle the two effects, we performed test calculations within the GW approximation keeping the screened Coulomb interaction fixed to its value at zero doping. The result is shown as
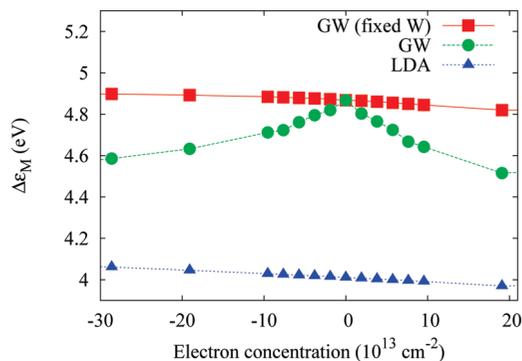
the green line in Figure 1. The doping dependence of the deformation potential is reduced by about a factor of 2. Therefore, we conclude that the role of the screening is comparable to the correction coming from the Green's function variation. In fact the shift of the Fermi level due to doping, leads to a suppression of transitions from π to π^* states. This affects the deformation potential through a change of both the screening and Green's function.

We compare the result for deformation potential with the one of the $\Delta\epsilon_M$ gap. For the latter we found that all the doping dependence is due to the screened Coulomb potential and not due to the change in the Green's function, see Figure 2, while in the first both effects contribute to the its behavior with doping. This is due to the fact that for the $K-A_1'$ phonon GW not only renormalizes the bare Green function lines but also introduces vertex corrections that behave different with the doping. However in general this is not true for other phonon modes, for instance, for the $\Gamma-E_{2g}$ mode vertex corrections have been proven to be negligible.[28]

At this point it is instructive to check the performance of DFT with hybrid functionals. We have performed calculations with the B3LYP functional.[39,40] Apart from an overestimation of $\langle D^2_{K}\rangle^{\pi\pi^*}_{k=0}$ by about 25 % (which could be corrected for by diminishing the percentage of Hartree−Fock exchange in the functional), the calculation reflects rather the doping dependence of the GW calculation with constant screening than the dependence of the full GW calculation. This can be understood, because the B3LYP functional contains screening on a very simplified level not suitable to describe extended systems and metals.

Now we want show how the variation of the deformation potential affects the Raman D peak dispersion and the splitting of the 2D line in multilayer graphene. The dispersion (peak energy versus laser frequency) of the Raman D and 2D lines in graphene is conveniently described by the double-resonant Raman model.[21] In order to calculate the phonon dispersion, we need the deformation potential for a phonon wavevector $K+q$ ($\langle D^2_{K+q}\rangle^{\pi\pi^*}_{k}$). In our earlier works we assumed this as a constant in q and k. The calculation for a finite q requires the use of very large supercells, which
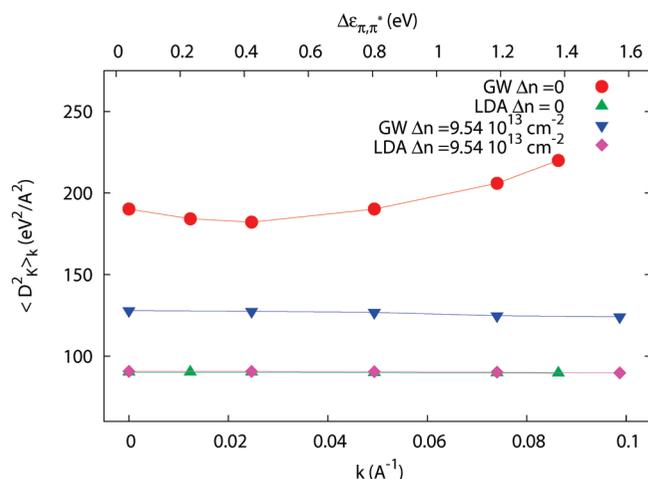
FIGURE 3. Square of the deformation potential, $\langle D^2_{K/k}\rangle^{\pi\pi*}$, with k varying along the line Γ−M, perpendicular to Γ−K. Four cases are reported: circles and up triangles are GW and LDA results for the undoped case; down triangles and rhombus are GW and LDA for high doping $\Delta n = 9.54 \times 10^{13}$ cm^{-2}. The upper labels refere to the corresponding electronic gap (the energy difference between π^* and π bands at K + k according to GW calculations at zero doping).

FIGURE 4. Change of slope of the Raman D peak dispersion versus doping. Arrows indicate the equivalent doping level for the KC_8, KC_{24}, and KC_{36} intercalated graphite.

are challenging for the GW approach. On the contrary, we can test the dependence of the deformation potential on the electron wavevector **k**. Indeed, we calculated $\langle D^2_{K/k}\rangle^{\pi\pi*}$ for **k** varying along the line **Γ−M**.[22] We found that $\langle D^2_{K/k}\rangle^{\pi\pi*}$ is almost constant in the doped case and it is slightly varying in the undoped one (within 10%), the result is reported in Figure 3. This finding justifies our previous assumption[27] of a constant square deformation potential that was also verified by direct comparison with the experiments.[8] In the double-resonant Raman model[21] the D-line dispersion is proportional to the phonon slope around **K** and thus proportional to $\langle D^2_{K/k}\rangle^{\pi\pi*}$. Furthermore, it is inversely proportional to the slope of the π/π^* bands and thus inversely proportional to $\Delta\epsilon_m$. In our previous work using the result at zero doping, we were able to reproduce completely ab initio the Raman D peak[27] dispersion (peak position versus laser frequency). With the information on the doping dependence of $\langle D^2_{K/k}\rangle^{\pi\pi*}$ and of $\Delta\epsilon_m$, we have calculated the Raman D peak dispersion as a function of the doping with the approach described in ref 27. In Figure 4 we report the resulting slope of the D-peak dispersion obtained as a linear fit of the dispersion between 1.0 and 3.2 eV laser energy. The D-peak dispersion is almost symmetric with respect to electron/hole doping, and it has its maximum at zero doping. Due to its strong variation with doping, it could be used also to detect experimentally the charge state of a graphene sample. Finally we suggest a simple way to verify our result in multilayer graphene using a single laser.[43] In multilayer graphene the 2D peak splits in different subpeaks and this splitting is proportional to the D-peak dispersion with the laser frequency.[11,12] Therefore we expect that mea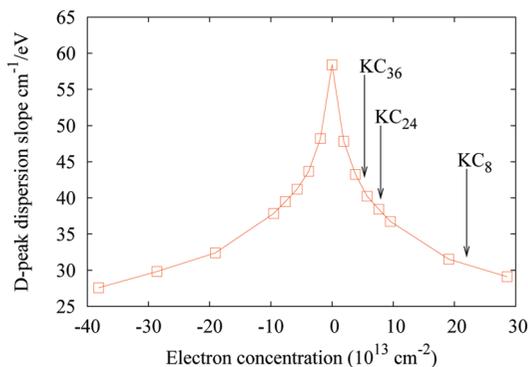surements of the 2D peak splitting as function of doping can highlight the strong variation of the D-peak dispersion, due to the squared deformation potential, as predicted in this work.

In conclusion, we have shown that in graphene $\langle D^2_{K/k}\rangle^{\pi\pi*}$ can be easily tuned with doping. This means that the electron and phonon interaction cannot be described by a simplified Hamiltonian with a fixed deformation potential as it is commonly done. Our findings can be easily verified experimentally by measuring the doping dependence of the Raman D peak dispersion, of the splitting of the 2D peak in multilayer graphene, and of the slope of the highest phonon branch close to **K**. The present findings open the possibility to use the slope of the D peak dispersion as a simple probe for the electrons/holes doping in graphene. The fact that the deformation potential is not a constant has implications also in the realization of graphene-based electronic devices where it is known that one of the limitations for ballistic transport is just the coupling between electrons and phonons.[3−5] Tuning electron−phonon coupling by doping could boost electronic properties of graphene-based devices. Concerning the puzzling discussion on the size of the EPC in graphene, our result puts another piece in support that EPC has to be larger than the LDA one and doping dependent. Finally, this new way to tune electron−phonon coupling can play a fundamental role in all the experiments where physical phenomena are directly related to doping as for instance the phonon renormalization,[6] phonon line width,[45] or the radiative decay of excitons in nanotubes.[46]

REFERENCES AND NOTES

(1)   Castro Neto, A. H.; Guinea, F.; Peres, N. M. R.; Novoselov, K. S.; Geim, A. K. *Rev. Mod. Phys.* **2009**, *81*, 109.

(2) Tsang; et al. *Nat. Nanotechnol.* **2007**, *2*, 725.

(3) Yao, Z.; et al. *Phys. Rev. Lett.* **2000**, *84*, 2941. Javey, A.; et al. *Phys. Rev. Lett.* **2004**, *92*, 106804.

(4) Lazzeri, M.; Piscanec, S.; Mauri, F.; Ferrari, A. C.; Robertson, J. *Phys. Rev. Lett.* **2005**, *95*, 236802. LeRoy, B. J.; Lemay, S. G.; Kong, J.; Dekker, C. *Nature (London)* **2004**, *432*, 371.

(5) Barreiro, A.; Lazzeri, M.; Moser, J.; Mauri, F.; Bachtold, A. *Phys. Rev. Lett.* **2009**, *103*, No. 076601.

(6) Kuzmenko, A. B.; Benfatto, L.; Cappelluti, E.; Crassee, I.; van der Marel, D.; Blake, P.; Novoselov, K. S. *Phys. Rev. Lett.* **2009**, *103*, 116804.

(7) Grüneis, A.; Attaccalite, C.; Rubio, A.; Vyalikh, D. V.; Molodtsov, S. L.; Fink, J.; Follath, R.; Eberhardt, W.; Büchner, B.; Pichler, T. *Phys. Rev. B* **2009**, *79*, 205106.

(8) Grüneis, A.; Serrano, J.; Bosak, A.; Lazzeri, M.; Molodtsov, S. L.; Wirtz, L.; Attaccalite, C.; Krisch, M.; Rubio, A.; Mauri, F.; Pichler, T. *Phys. Rev. B* **2009**, *80*, No. 085423.

(9) Li, Guohong; Luican, Adina; Andrei, Eva Y. *Phys. Rev. Lett.* **2009**, *102*, 176804.

(10) Das, A.; et al. *Nat. Nanotechnol.* **2008**, *3*, 210. Das, A. *Phys. Rev. B* **2009**, *79*, 155417.

(11) Ferrari, A. C.; Meyer, J. C.; Scardaci, V.; Casiraghi, C.; Lazzeri, M.; Mauri, F.; Piscanec, S.; Jiang, D.; Novoselov, K. S.; Roth, S.; Geim, A. K. *Phys. Rev. Lett.* **2006**, *97*, 187401.

(12) Graf, D.; Molitor, F.; Ensslin, K.; Stampfer, C.; Jungen, A.; Hierold, C.; Wirtz, L. *Nano Lett.* **2007**, *7*, 238.

(13) Pisana, S.; Lazzeri, M.; Casiraghi, C.; Novoselov, K. S.; Geim, A. K.; Ferrari, A. C.; Mauri, F. *Nat. Mater.* **2007**, *6*, 198.

(14) Yan, J.; Zhang, Y.; Kim, P.; Pinczuk, A. *Phys. Rev. Lett.* **2007**, *98*, 166802.

(15) Casiraghi, C.; Pisana, S.; Novoselov, K. S.; Geim, A. K.; Ferrari, A. C. *Appl. Phys. Lett.* **2007**, *91*, 233108.

(16) Stampfer, C.; Molitor, F.; Graf, D.; Ensslin, K.; Jungen, A.; Hierold, C.; Wirtz, L. *Appl. Phys. Lett.* **2007**, *91*, 241907.

(17) Basko, D. M.; Piscanec, S.; Ferrari, A. C. *Phys. Rev. B* **2009**, *80*, 165413.

(18) Lazzeri, M.; Mauri, F. *Phys. Rev. Lett.* **2006**, *97*, 266407.

(19) Casiraghi, C.; Hartschuh, A.; Qian, H.; Piscanec, S.; Georgi, C.; Novoselov, K. S.; Basko, D. M.; Ferrari, A. C. *Nano Lett.* **2009**, *9*, 1433.

(20) Matteo, Calandra; Francesco, Mauri *Phys. Rev. B* **2007**, *76*, 205411.

(21) Thomsen, C.; Reich, S. *Phys. Rev. Lett.* **2000**, *85*, 5214.

(22) We consider $\mathbf{k}$ along the line $\Gamma-\mathbf{M}$, perpendicular to $\Gamma-\mathbf{K}$, of the graphene unit cell. $\langle D_{\mathbf{K}}^2 \rangle_{\mathbf{K}}^{\pi\pi^*}$ can be obtained from the band energies of a $\sqrt{3} \times \sqrt{3}$ supercell (see Figure 3b of ref 27). The two Dirac cones at $\mathbf{K}$ and $2\mathbf{K}$ of the unit cell are refolded at Γ in the supercell. We dispalce each atom by d, following the $\mathbf{K}-A'_1$ phonon pattern. We define $\Delta\epsilon_d(\mathbf{k}) = \bar{\epsilon}_{\pi^*}(\mathbf{k}) - \bar{\epsilon}_{\pi}(\mathbf{k})$, where $\bar{\epsilon}_{\pi^*}$ ($\bar{\epsilon}_\pi$) is the average between the energy of the two π^* (π) bands corresponding to $\mathbf{K} + \mathbf{k}$ and $2\mathbf{K} + \mathbf{k}$ of the unit cell $\langle D_{\mathbf{K}}^2 \rangle_{\mathbf{K}}^{\pi\pi^*} = (\Delta\epsilon_d(\mathbf{k}))^2 - (\Delta\epsilon_0(\mathbf{k}))^2/(8d^2)$.

(23) Piscanec, S.; Lazzeri, M.; Mauri, F.; Ferrari, A. C.; Robertson, J. *Phys. Rev. Lett.* **2004**, *93*, 185503.

(24) Ishikawa, K.; Ando, T. *J. Phys. Soc. Jpn.* **2006**, *75*, No. 084713.

(25) Saha, S. K.; Waghmare, U. V.; Krishnamurthy, H. R.; Sood, A. K. *Phys. Rev. B* **2007**, *76*, 201404.

(26) Tse, W. K.; Das Sarma, S. *Phys. Rev. Lett.* **2007**, *99*, 236802.

(27) Lazzeri, M.; Attaccalite, C.; Wirtz, L.; Mauri, F. *Phys. Rev. B* **2008**, *78*, No. 081406(R).

(28) Basko, D. M.; Aleiner, I. L. *Phys. Rev. B* **2008**, *77*, No. 041409(R).

(29) Grüneis, A.; Attaccalite, C.; Rubio, A.; Vyalikh, D. V.; Molodtsov, S. L.; Fink, J.; Follath, R.; Eberhardt, W.; Büchner, B.; Pichler, T. *Phys. Rev. B* **2009**, *80*, No. 075431.

(30) In all DFT calculations the distance between the graphene planes was 20 a.u., the Brillouin zone integration was performed using an uniform k-point grid $36 \times 36 \times 1$, with the functional of ref 47, plane waves (60 Ry cut-off) and pseudopotentials,[48] using the PWSCF code.[49] An electronic smearing of 0.02 Ry with the Fermi−Dirac distribution was employed.

(31) Lazzeri, M.; Mauri, F. *Phys. Rev. Lett.* **2006**, *97*, 266407.

(32) Park, C. H.; Giustino, F.; Cohen, M. L.; Louie, S. G. *Phys. Rev. Lett.* **2007**, *99*, No. 086804.

(33) Grüneis, A.; et al. *Phys. Rev. B* **2008**, *78*, 205425.

(34) Non-self-consistent GW calculations have been performed starting from DFT-LDA wavefunctions, using a plasmon pole approximation, following the scheme of Hybertsen and Louie,[35] with the code YAMBO.[50] We use a $36 \times 36 \times 1$ k-point grid for the primitive cell and an equivalent one for the supercell. Convergence in the number of bands and size of the dielectric constant has been carefully checked.

(35) Hybertsen, M. S.; Louie, S. G. *Phys. Rev. B* **1986**, *34*, 5390.

(36) Zhou, S. Y.; et al. *Nat. Phys.* **2006**, *2*, 595–599.

(37) Grüneis, A.; et al. *Phys. Rev. Lett.* **2008**, *100*, No. 037601.

(38) Notice that nonadiabatic corrections, not considered here, are though to be important for the G phonon but not for the $\mathbf{K}$ phonon, see ref 31.

(39) Becke, A. D. *J. Chem. Phys.* **1993**, *98*, 5648.

(40) For the B3LYP calculat ions we used the code CRYSTAL (Saunders, V. R., et al.; Dovesi, R.; Roetti, C.; Orlando, R.; Zicovich-Wilson, C. M.; Harrison, N. M.; Doll, K.; Civalleri, B.; Bush, I. J.; D'Arco, Ph.; Llunell, M. *CRYSTAL03 User's Manual*: University of Torino: Torino, 2003),using the TZ basis by Dunning (without the diffuse P-function). K-point sampling and thermal smearing are the same as in the GW calculations.

(41) Polini, M.; Asgari, R.; Barlas, Y.; Pereg-Barnea, T.; MacDonald, A. H. *Solid State Commun.* **2007**, *143*, 58.

(42) Attaccalite, C.; Rubio, A. *Phys. Status Solidi B* **2009**, *246*, 2523.

(43) We suppose that is the case also in multilayer graphene, althougt the band structure is different from that graphene, a result similar to the one we found for graphen holds, as we found for graphite.[27]

(44) Faugeras, C.; Amado, M.; Kossacki, P.; Orlita, M.; Sprinkle, M.; Berger, C.; de Heer, W. A.; Potemski, M. *Phys. Rev. Lett.* **2009**, *103*, 186803.

(45) Park, C. H.; Giustino, F.; Cohen, M. L.; Louie, S. G. *Nano Lett.* **2008**, *8*, 4229.

(46) Perebeinos, V.; Avouris, P. *Phys. Rev. Lett.* **2008**, *101*, No. 057401.

(47) Ceperley, D. M.; Alder, B. J. *Phys. Rev. Lett.* **1980**, *45*, 566.

(48) Troullier, N.; Martins, J. L. *Phys. Rev. B* **1991**, *43*, 1993.

(49) Giannozzi, P.; et al. *J. Phys.: Condens. Matter* **2009**, *21*, 395502. (http://www.quantum-espresso.org).

(50) Marini, A.; Hogan, C; Gruning, M.; Varsano, D. *Comput. Phys. Commun.* **2009**, *180*, 1392. (http://www.yambo-code.org).